Free Radical Research, June 2007; 41(6): 638–644

informa
healthcare

Ursolic acid regulates high glucose-induced apoptosis

CHANG JOO OH[1], IN SUP KIL[1], CHAN IK PARK[2], CHAE HA YANG[2], & JEEN-WOO PARK[1]

[1]*School of Life Sciences and Biotechnology, College of Natural Sciences, Kyungpook National University, Taegu 702-701, South Korea, and* [2]*Daegu Haany University, Taegu 706-828, South Korea*

Accepted by Professor J. Yodoi

(Received 15 September 2006; in revised form 28 December 2006)

Abstract
A high concentration of glucose has been implicated as a causal factor in initiation and progression of diabetic complications and there is evidence to suggest that hyperglycemia increases the production of free radicals and oxidative stress. Therefore, compounds that scavenge reactive oxygen species (ROS) may confer regulatory effects on high glucose-induced apoptosis. Ursolic acid (UA), a pentacyclic triterpene, is reported to have an antioxidant activity. We investigated the effect of UA on high glucose-induced apoptosis in U937 cells. Upon exposure to 35 mM glucose for two days, there was a distinct difference between untreated cells and cells pre-treated with 50 nM UA for 2 h in regard to cellular redox status and oxidative DNA damage to cells. UA pre-treated cells showed significant suppression of apoptotic features such as DNA fragmentation, damage to mitochondrial function and modulation of apoptotic marker proteins upon exposure to high glucose. This study indicates that UA may play an important role in regulating the apoptosis induced by high glucose presumably through scavenging of ROS.

Keywords: *Ursolic acid, apoptosis, diabetes, antioxidant*

Introduction

Autoxidation of sugars and of the products of nonenzymatic glycation of proteins is a free radical-mediated reaction that occurs under aerobic conditions. It has been suggested that oxidative stress induced by hyperglycemia is a key factor in the pathogenesis of diabetic complications [1–5]. The glycation proceeds through the formation of a Schiff base between the carbonyl group of sugar and an α- or ε-amino group in a protein together with Amadori rearrangement to yield a relatively stable ketoamine [6,7]. Such a reaction has been expected to occur in various kinds of proteins under physiological conditions. Recently, it has been proposed that generation of reactive oxygen species (ROS) and accumulation of advanced glycation end products (AGE) trigger apoptosis in renal cells in diabetic hyperglycemia [8,9].

There has been an increased interest in herbal and natural products which protect diabetic complications. Ursolic acid (UA), a pentacyclic triterpene acid, has been isolated from many kinds of medicinal plants, such as *Eriobotrya japonica*, *Rosmarinns officinalis*, *Melaleuca leucadendron*, *Ocimum sanctum* and *Glechoma hederaceae*. UA has been reported to produce antitumor activities and antioxidant activity [10].

In the present report, we demonstrate that UA exhibits the regulatory role in U937 cells against apoptosis induced by a high concentration of glucose. These results suggest that UA has an important protective role in hyperglycemia-induced apoptosis, presumably, through acting as an antioxidant.

Correspondence: J.-W. Park, School of Life Sciences and Biotechnology, College of Natural Sciences, Kyungpook National University, Taegu 702-701, South Korea. Fax:82 53 943 2762. E-mail: parkjw@knu.ac.kr

ISSN 1071-5762 print/ISSN 1029-2470 online © 2007 Informa UK Ltd.
DOI: 10.1080/10715760701227526

Materials and methods

Materials

D-Glucose, UA, propidium iodide (PI), 4′,6-diamidino-2-phenylindole (DAPI), diphenylamine and xylenol orange were purchased from Sigma Chemical Company (St Louis, MO). 2′,7′-dichlorofluorescin diacetate (DCFH-DA), dihydrorhodamine (DHR) 123 and rhodamine 123 dye were purchased from Molecular Probes (Eugene, OR). Electrophoreses reagents and Bio-Rad protein assay kit were purchased from Bio-Rad (Hercules, CA). Antibodies were purchased from Santa Cruz (Santa Cruz, CA).

Cell culture

Human permonocytic U937 cells (American Type Culture Collection, Rockville, MD) were grown in RPMI 1640 culture medium supplemented with 10% (v/v) FBS and penicillin (50 U/ml) and streptomycin (50 μg/ml) at 37°C in a 5% CO_2–95% air humidified incubator.

Immunoblot analysis

Proteins were separated on 10% SDS-polyacrylamide gel, transferred to nitrocellulose membranes and subsequently subjected to immunoblot analysis using appropriate antibodies. Immunoreactive antigen was then recognized by using horseradish peroxidase-labeled anti-rabbit IgG and an enhanced chemiluminescence detection kit (Amersham Pharmacia Biotech).

DAPI staining

DAPI staining was used for apoptotic nuclei determination. U937 cells were collected at 2000*g* for 5 min, washed once with cold PBS, fixed in ice-cold methanol/acetic acid (1:1, v/v) for 5 min and stained with 0.8 μg/ml DAPI in the dark state. The morphological changes of apoptotic cells were analyzed by the Zeiss Axiovert 200 microscope at fluorescence DAPI region (excitation, 351 nm; emission, 380 nm).

DNA fragmentation

DNA ladder formation assay was performed by an agarose gel electrophoresis. DNA fragmentation was also determined using the diphenylamine assay as previously described [11]. Cells were collected by centrifugation, resuspended in 250 μl 10 mM Tris and 1 mM EDTA, pH 8.0 (TE buffer) and incubated with one additional volume of lysis buffer (5 mM Tris, 20 mM EDTA and 0.5% Triton X-100, pH 8.0) for 30 min at 4°C. After lysis, the intact chromatin (pellet) was separated from DNA fragments (supernatant) by centrifugation for 15 min at 13,000*g*. Pellets were resuspended in 500 μl TE buffer and samples were precipitated by adding 500 μl 10% trichloroacetic acid at 4°C. Samples were pelleted at 4000*g* for 10 min and the supernatant was removed. After addition of 300 μl 5% trichloroacetic acid, samples were boiled for 15 min. DNA content was quantitated using the diphenylamine reagent. The percentage of fragmented DNA was calculated as the ratio of the DNA content in the supernatant to the amount in the pellet.

FACS

To determine the portion of apoptotic cells, cells were analyzed with propidium iodide (PI) staining [12]. U937 cells were collected at 2000*g* for 5 min and washed once with cold PBS, fixed in 70% ethanol, decant ethanol by centrifuge and stained with 1 ml of solution containing 50 mg/ml PI, 1 mg/ml RNase A, 1.5% Triton X-100 for at least 1 h in the dark at 4°C. Labeled nuclei were subjected to flow cytometric analysis and then gated on light scatter to remove debris and the percentage of nuclei with a sub-G_1 content was considered apoptotic cells.

Intracellular ROS

Hydrogen peroxide oxidizes ferrous (Fe^{2+}) to ferric ion (Fe^{3+}) selectively in dilute acid and the resulting ferric ions can be determined using a ferric sensitive dye, xylenol orange, as an indirect measure of hydrogen peroxide concentration. The cell extracts were added to FOX solution (0.1 mM xylenol orange, 0.25 mM ammonium ferrous sulfate, 100 mM sorbitol and 25 mM H_2SO_4) and incubated in a room temperature for 30 min and absorbance was measured at 560 nm. Hydrogen peroxide was used to draw standard curve as described [13]. Intracellular peroxide production was measured using DCFH-DA as described [14].

Oxidative DNA damage

8-Hydroxy-2′-deoxyguanosine (8-OH-dG) levels of U937 cells were estimated by using a fluorescent binding assay as described by Struthers et al. [15]. After U937 cells were exposed to high glucose, cells were fixed and permeabilized with ice-cold methanol for 15 min. DNA damage was visualized with avidin-conjugated TRITC (1:200 dilution) for fluorescent microscope with 540 nm excitation and 588 nm emission.

Mitochondrial damage

Mitochondrial membrane potential transition (MPT) was measured by the incorporation of rhodamine 123 dye into the mitochondria, as previously described [16]. Cells (1×10^6) grown on poly-L-lysine coated slide glasses were exposed to high glucose. Cells were then treated with 5 μM rhodamine 123 for 15 min and

excited at 488 nm with an argon laser. Cells were double-stained with 100 nM MitoTracker Red, which is a morphological marker of mitochondria. The fluorescence images at 520 nm were simultaneously obtained with a laser confocal scanning microscope. To evaluate the levels of mitochondrial ROS, U937 cells in PBS were incubated for 20 min at 37°C with 5 μM DHR 123 and cells were double-stained with 100 nM MitoTracker Red. DHR 123 and MitoTracker Red fluorescence was visualized with a fluorescence microscope.

Quantitation of relative fluorescence

The averages of fluorescence intensity from fluorescence images were calculated as described [17].

Replicates

Unless otherwise indicated, each result described in the paper is representative of at least three separate experiments.

Results

The effects of high glucose and UA on the cellular markers of apoptosis were studied to determine whether these would correlate with changes in the apoptotic pathways. When U937 cells were treated with 35 mM glucose for two days, shrinkage of the cell and plasma membrane blebbing was apparently observed by light microscopy (data not shown). To assess whether these changes were attributable to apoptotic changes, nuclear morphology was assessed by fluorescence microscopy using DAPI. As shown in Figure 1(A), nuclear condensation and fragmentation were apparent in U937 cells exposed to high glucose. However, cells pre-treated with 50 nM UA for 2 h were significantly more resistant than untreated cells to high glucose-induced apoptosis. UA by itself did not induced apoptosis at this concentration. Figure 1(B) shows a typical cell cycle plot of U937 cells that were unexposed or exposed to 35 mM glucose for two days. Apoptotic cells were estimated by calculating the number of subdiploid cells in the

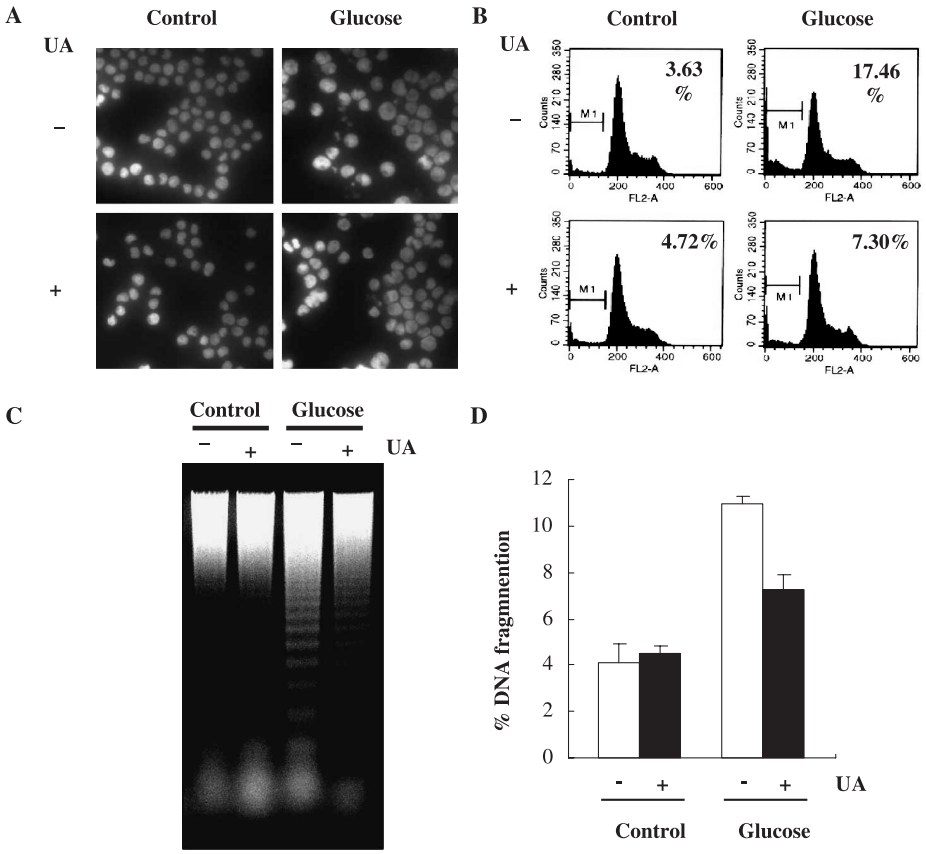

Figure 1. Effects of UA on high glucose-induced DNA fragmentation in U937 cells. (A) High glucose-induced nuclear condensation and fragmentation in U937 cells. UA (50 nM, 2 h)-pretreated and untreated U937 cells were exposed to 35 mM glucose for two days and then harvested, fixed, permeabilized and loaded with 0.8 μg/ml DAPI for 5 min. The morphological changes of cells were analyzed by fluorescence microscopy (excitation, 351 nm; emission, 380 nm). (B) Cell cycle analysis with cellular DNA content was examined by flow cytometry. The sub-G_1 region (presented as "M1") includes cells undergoing apoptosis. The number of each panel refers to the percentage of apoptotic cells. (C) Agarose gel electrophoresis of nuclear DNA fragments of U937 cells exposed to 35 mM glucose for two days, showing the ladder pattern characteristic of apoptosis. (D) DNA fragmentation was determined using diphenylamine assay. The results shown are the means ± SD of three separate experiments.

cell cycle histogram. When cells were exposed to glucose, apoptotic cells were increased markedly in untreated cells as compared to UA-treated cells.

High glucose-triggered apoptosis in U937 cells was determined by the measurement of DNA fragmentation using agarose gel electrophoresis (Figure 1(C)). DNA fragmentation was further confirmed by the diphenylamine assay (Figure 1(D)). The DNA fragmentation was significantly reduced in UA-treated cells compared to untreated cells upon exposure to 35 mM glucose for two days.

To investigate whether the difference in apoptotic cell death of U937 cells upon exposure to high glucose is associated with ROS formation, the levels of intracellular peroxides in the U937 cells were evaluated by confocal microscopy with the oxidant-sensitive probe DCFH-DA. As shown in Figure 2(A), an increase in DCF fluorescence was observed in U937 cells when they were exposed to 35 mM glucose for two days. The increase in fluorescence was significantly reduced in cells pre-treated with 50 nM UA for 2 h. We also demonstrated the level of intracellular H_2O_2 in cells irradiated in the presence and absence of UA. The pre-treatment of UA resulted in a significantly lower intracellular level of H_2O_2 as compared to that of untreated cells with the exposure of 35 mM glucose for two days (Figure 2(B)). These data strengthen the conclusion that UA provided protection from the high glucose-induced apoptosis by decreasing the steady-state level of intracellular oxidants. 8-OH-dG, the most abundant and most studied lesion in DNA generated by intracellular ROS, has been used as an indicator of oxidative DNA damage *in vivo* and *in vitro* [18]. Recently, it has been shown that 8-OH-dG level is specifically measured by a fluorescent binding assay using avidin-conjugated TRITC [15]. The fluorescent intensity which reflects the endogenous levels of 8-OH-dG in DNA was significantly increased in cells upon exposure to high glucose. In contrast, the overall DNA appeared to be markedly protected in UA-treated cells even after exposure to the same dose of glucose (Figure 2(C)). These results indicate that UA appears to protect cells from oxidative DNA damage caused by high glucose.

Alterations in mitochondrial integrity and function may play an important role in the apoptotic cascade. MPT, associated with the opening of large pores in the mitochondrial membranes, is a very important event in apoptosis and ROS is one of the major stimuli that change MPT [19]. To answer whether UA modulates the MPT upon exposure to high glucose, we determined the change in MPT by intensity of fluorescence emitting from a lipophilic cation dye, rhodamine 123. Significantly less rhodamine 123 dye was taken up by the mitochondria of untreated cells, compared with UA-treated cells (Figure 3(A) and (B)). To determine if changes in MPT were accompanied by changes in intracellular ROS, The levels of intracellular peroxides in the mitochondria of U937 cells were evaluated by confocal microscopy with the oxidant-sensitive probe DHR 123. As shown in Figure 3(C), the intensity of fluorescence was significantly lower in cells pre-treated with 50 nM UA for 2 h when compared to that in the mitochondria of untreated cells when U937 cells were exposed to 35 mM glucose for two days. These results indicate that high glucose most likely leads to increased mitochondrial injury while UA protects mitochondria from oxidative damage.

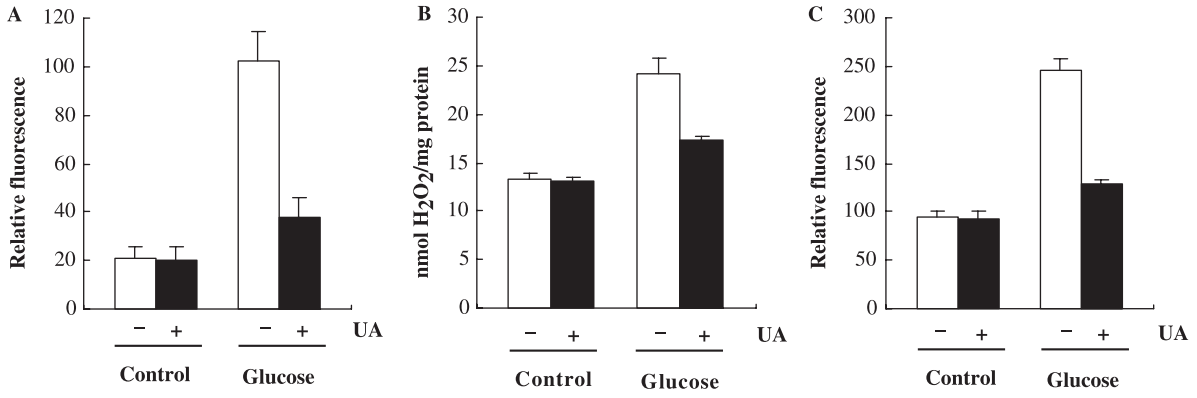

Figure 2. (A) Measurement of *in vivo* molecular oxidation. DCF fluorescence was measured in U937 cells exposed to high glucose. Fluorescence was recorded at an excitation wavelength of 504 nm and an emission wavelength of 524 nm. The average of fluorescence intensity was calculated as described [17]. The results shown are the means ± SD of five separate experiments. (B) Production of hydrogen peroxide in U937 cells exposed to high glucose was determined by the method described under Materials and Methods. The results shown are the means ± SD of five separate experiments. (C) 8-OH-dG levels reflected by the binding of avidin-TRITC were visualized by a fluorescence microscope with 488 nm excitation and 580 nm emission. The average of fluorescence intensity was calculated as described [17]. The results shown are the means ± SD of three separate experiments.

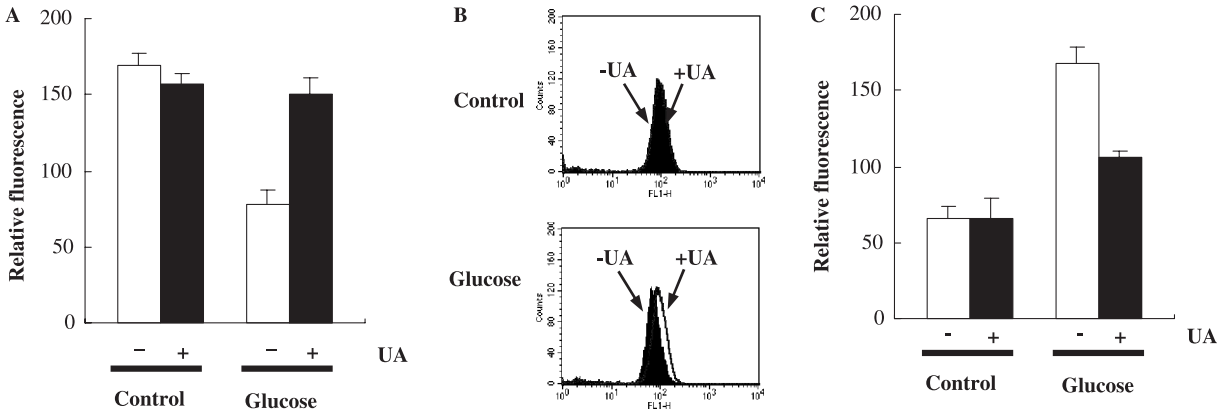

Figure 3. (A) MPT of U937 cells was measured by the incorporation of rhodamine 123 dye into the mitochondria. The average of fluorescence intensity was calculated as described [17]. The results shown are the means ± SD of three separate experiments. (B) FACS analysis of rhodamine 123 fluorescence. (C) DHR 123 was employed to detect mitochondrial ROS. DHR 123 fluorescence was visualized by a fluorescence microscope. The average of fluorescence intensity was calculated as described [17]. The results shown are the means ± SD of three separate experiments.

We evaluated changes in the apoptotic marker proteins as a result of high glucose and the influence of UA on these proteins. Caspase-3 and caspase-8 activation in U937 cells was assessed by immunoblot analysis of lysates from cells that had been exposed to 35 mM glucose for two days, with and without UA (Figure 4). High glucose induced cleavage of caspase-3 and caspase-8, however, the cleavage was significantly reduced by UA. High glucose also induced the formation of fragments which represents proteolytic cleavage of PARP and lamin B, indicates an oncoming apoptotic process. The cleaved products of PARP and lamin B increased markedly in untreated cells compared to UA pre-treated cells upon exposure to high glucose (Figure 4). Taken together, high glucose-induced cleavage of procaspase-3 into the active form of caspase-3 and caspase-3 induces degradation of PARP or lamin B. The results also indicate that UA exhibits a protective effect on the high glucose-induced apoptosis. We determined the changes in levels of the p53 tumor suppressor protein, which leads either to cell cycle arrest and repair or to apoptosis. The results in Figure 4 compare the changes in p53 in U937 cells induced by high glucose with and without UA. Levels of p53 increased as a result of high glucose treatment and UA inhibited the high glucose-induced change in p53 levels. Activation of JNK has been implicated in inducing apoptosis in response to environmental stimuli. As shown in Figure 4, the activation of JNK induced by high glucose was significantly inhibited by UA. In contrast, the activation of ERK 1/2, which have been known to be involved in cell survival, significantly enhanced by UA. We determined the effect of UA on high glucose-induced nuclear translocation of p65 to demonstrate that anti-apoptotic effect of UA may be mediated in part through the suppression of the NF-κB activation pathway. High glucose induced the translocation of p65 and UA suppressed it. Because IκBα degradation is required for activation of NF-κB, we determined whether inhibition of high glucose-induced NF-κB activation by UA was because of

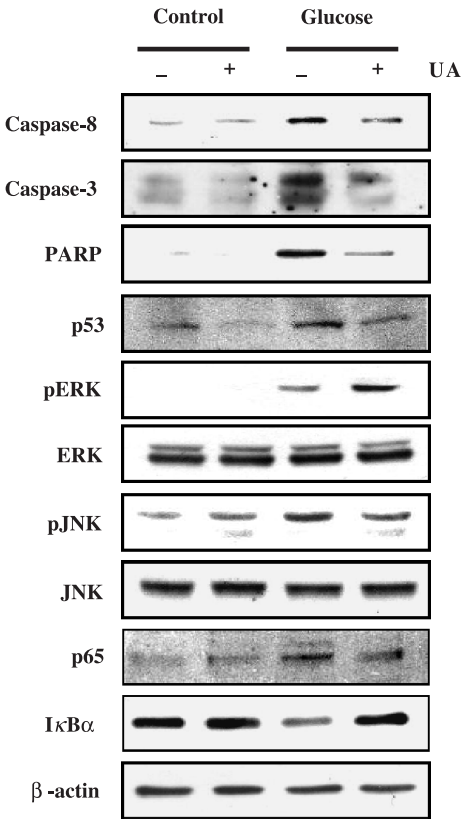

Figure 4. Immunoblot analysis of various apoptosis-related proteins in U937 cells unexposed or exposed to 35 mM glucose for two days. Cell extracts were subjected to 10–12.5% SDS-PAGE and immunoblotted with antibodies against cleaved caspase-3, cleaved caspase-8, cleaved PARP, p53, phospho-ERK, ERK, phospho-JNK, JNK, p65 and IκBα. β-Actin was run as an internal control.

inhibition of IκBα degradation. We found that high glucose-induced IκBα degradation in untreated cells, but in UA-pretreated cells high glucose had no significant effect on IκBα degradation.

Discussion

Both AGE accumulation and oxidative stress involved in the pathogenesis of diabetic complications such as nephropathy, retinopathy and neuropathy [1,20]. Prevention of synthesis and tissue accumulation of AGE- or oxidative-derived end products could constitute a major advance in the treatment of diabetic complications. Our observations are consistent with the hypothesis that ROS play a pivotal role in apoptosis and that reductants can block or delay this process [21]. In the present study, we examined the apoptotic pathway initiated by high glucose in U937 cells. The perturbation of redox status reflected by the modulation of intracellular ROS generation, MPT alteration, caspase-3 activation, cleavage of caspase target proteins and DNA fragmentation were observed. The pre-treatment of UA significantly improved redox status and inhibited the whole apoptotic pathway. Several mechanisms may interplay in the protective effect of UA. The present results indicate that antioxidant effects of UA may be responsible for its anti-apoptotic effect against high glucose.

Mitochondria are vulnerable to oxidants because they are the major source of free radicals in the cells and are limited in their ability to cope with oxidative stress [22]. Therefore, improving the mitochondrial status could cause a significant decrease in the level of oxidants in the cells [23]. The involvement of mitochondria in apoptosis has been extensively discussed [24]. The changes caused by high glucose are compatible with mitochondrial failure, encompassing generation of ROS and accumulation of rhodamine 123 which reflect mitochondrial swelling or changes in the mitochondrial inner membrane. A clear suppression of such damages indicates that UA prevents a deterioration of bioenergetic state.

Cleavage of caspase-3 and its target proteins such as PARP and lamin B, a signature event of apoptosis, was induced by high glucose. Wild-type p53 tumor suppressor protein has been shown to be functionally necessary for growth inhibition and apoptosis following exposure to oxidative stress [25]. Levels of p53 were increased in U937 cells after exposure to high glucose. The presence of UA inhibited the high glucose-induced increase in p53 levels. NF-κB is a family of Rel domain-containing proteins present in the cytoplasm of all cells. Under resting conditions, NF-κB consists of a heterodimer of p50, p65 and IκBαin the cytoplasm; only when activated and translocated in the nucleus in the sequence of events leading to activation initiated [26]. The translocation of p65 and degradation of IκBα induced by high glucose were inhibited by UA. It has been known that NF-κB is activated by ROS and various cellular stresses related to ROS generation, such as inflammation, ionizing radiation, heat shock and presumably hyperglycemia. In this regard, it can be assumed that antioxidant capacity of UA may responsible for the suppression of NF-κB activation. It has recently been reported that UA alone induces ERK 1/2 phosphorylation in RAW 264.7 mouse macrophages and NF-κB activation in mouse resting macrophages. However, our results show that UA suppresses NF-κB activation in U937 cells under exposure to high glucose. There is mounting evidence that human monocytic U937 cells are highly susceptible to many types of stresses. They also have variety of functions against external stress [27]. This apparent difference in the cellular response to oxidative stress and antioxidants including UA presumably depend on cell types. It remains to be studied and thus determined the factors attributed difference in the cell-specific responses.

In conclusion, the present study demonstrates that UA abrogates the high glucose-induced early production of ROS, leading to protection against apoptotic cell death.

Acknowledgements

This work was supported by a grant (R12-2003-002-04002-0) from the basic science program of the Ministry of Commerce, Industry and Energy.

References

[1] Brownlee M. Biochemistry and molecular cell biology of diabetic complications. Nature 2000;414:813–820.
[2] Nishikawa T, Edelstein D, Brownlee M. The missing link: A single unifying mechanism for diabetic complications. Kidney Int 2000;58:26–30.
[3] Nishikawa T, Edelstein D, Du XL, Yamagishi S, Matsumura T, Kaneda Y, Yorek MA, Beebe D, Oates PJ, Hammes HP, Giardino I, Brownlee M. Normalizing mitochondrial superoxide production blocks three pathways of hyperglycaemic damage. Nature 2001;404:787–790.
[4] Vincent MA, Brownlee M, Russell JW. Oxidative stress and programmed cell death in diabetic neuropathy. Ann NY Acad Sci 2002;959:368–383.
[5] Kiritoshi S, Nishikawa T, Sonoda K, Kukidome D, Senokuchi T, Matsuo T, Matsumura T, Tokunaga H, Brownlee M, Araki E. Reactive oxygen species from mitochondria induce cyclooxygenase-2 gene expression in human mesangial cells: Potential role in diabetic nephropathy. Diabetes 2003;52:2570–2577.
[6] Wolff SP, Dean RT. Glucose autoxidation and protein modification. The potential role of 'autoxidative glycosylation' in diabetes. Biochem J 1987;245:243–250.
[7] Azevedo M, Falcao J, Raposo J, Manso C. Superoxide radical generation by Amadori compounds. Free Radic Res Commun 1988;4:331–335.
[8] Yamagishi S, Inagaki Y, Okamoto T, Amano S, Koga K, Takeuchi M, Aakita Z. Advanced glycation end product-induced apoptosis and overexpression of vascular endothelial growth

factor and monocyte chemoattractant protein-1 in human-cultured mesangial cells. J Biol Chem 2002;277:20309–20315.
[9] Allen DA, Harwood S, Varagunam M, Raftery MJ, Yaqoob MM. High glucose-induced oxidative stress causes apoptosis in proximal tubular epithelial cells and is mediated by multiple caspases. FASEB J 2003;17:908–910.
[10] Aggarwal BB, Shishodia S. Molecular targets of dietary agents for prevention and therapy of cancer. Biochem Pharmacol 2006;71:1397–1421.
[11] Williams JM, Lea N, Lord JM, Roberts LM, Milford DV, Taylor CM. Comparison of ribosome-inactivating proteins in the induction of apoptosis. Toxicol Lett 1997;91:121–127.
[12] Darzynkiewicz Z, Sharpless T, Staiano-Coico L, Melamed MR. Sub-compartments of the G_1 phase of cell cycle detected by flow cytometry. Proc Natl Acad Sci USA 1980;77:6696–6699.
[13] Jiang ZY, Hunt JV, Wolff SP. Ferrous ion oxidation in the presence of xylenol orange for detection of lipid hydroperoxide in low density lipoprotein. Anal Biochem 1992;202:384–389.
[14] Royall JA, Ischiropoulos H. Evaluation of 2′,7′-dichlorofluorescin and dihydrorhodamine 123 as fluorescent probes for intracellular H_2O_2 in cultured endothelial cells. Arch Biochem Biophys 1993;302:348–355.
[15] Struthers I, Patel R, Clark J, Thomas S. Direct detection of 8-oxodeoxyguanosine and 8-oxoguanine by avidin and its analogues. Anal Biochem 1998;255:20–31.
[16] Pastorino JG, Simbula G, Yamamoto K, Glascott PA, Rothman RJ, Farber JL. The cytotoxicity of tumor necrosis factor depends on induction of the mitochondrial permeability transition. J Biol Chem 1996;271:29792–29798.
[17] Sundaresan M, Yu ZY, Ferrans CJ, Irani K, Finkel T. Requirement for generation of H_2O_2 for platelet-derived growth factor signal transduction. Science 1995;270:296–299.
[18] Park JW, Floyd RA. Lipid peroxidation products mediate the formation of 8-hydroxydeoxyguanosine in DNA. Free Radic Biol Med 1992;12:245–250.
[19] Kroemer G, Zamzami N, Susin SA. Mitochondrial control of apoptosis. Immunol Today 1997;18:44–51.
[20] Baynes JW. Role of oxidative stress in development of complications in diabetes. Diabetes 1991;40:405–412.
[21] Kannan K, Jain SK. Oxidative stress and apoptosis. Pathophysiology 2000;7:153–163.
[22] de Grey AD. The reductive hotspot hypothesis: An update. Arch Biochem Biophys 2000;373:295–301.
[23] Atamna H, Paler-Martinez A, Ames BN. *N-t*-Butylhydroxylamine, a hydrolysis product of α-phenyl-*N-t*-butylnitrone, is more potent in delaying senescence in human lung fibroblasts. J Biol Chem 2000;275:6741–6748.
[24] Green DR, Reed JC. Mitochondria and apoptosis. Science 1998;281:1309–1312.
[25] Kastan MB, Onyekwere O, Sidransky D, Vogelstein B, Craig RW. Participation of p53 protein in the cellular response to DNA damage. Cancer Res 1991;51:6304–6311.
[26] Sethi G, Ahn KS, Sandur SK, Lin X, Chaturvedi MM, Aggaewal BB. Indirubin enhances tumor necrosis factor-induced apoptosis through modulation of nuclear factor-κB signaling pathway. J Biol Chem 2006;281:23425–23435.
[27] Lee JH, Park JW. The effect of α-phenyl-*N-t*-butylnitrone on ionizing radiation-induced apoptosis in U937 cells. Free Radic Res 2005;39:1325–1333.